STEREO EVALUATION OF CARTOSAT-1 DATA ON TEST SITE 5 - FIRST DLR RESULTS

Manfred Lehner, Rupert Müller, Peter Reinartz

German Aerospace Center (DLR), Remote Sensing Technology Institute, D-82234 Wessling, Germany

CARTOSAT-1 Scientific Assessment Program – Commission IV

ABSTRACT:

DLR's Remote Sensing Technology Institute has more than 20 years of history in developing spaceborne stereo scanners (MEOSS, MOMS) and the corresponding stereo evaluation software systems. The institute takes part in CARTOSAT-1 Scientific Assessment Program (C-SAP) as a principal investigator for German (Southeast Bavaria, test site not yet included in the C-SAP list) and Spanish (Catalonia, TS10) test sites for which also PI evaluations for SPOT-5 HRS SAP had been done in 2003-4.
As CARTOSAT-1 data of Catalonia (test site 10) did not correspond to the available ground truth, negotiations with ICC brought forward a new fitting set of ground truth. Unfortunately, this new reference data came too late for phase I of C-SAP. Thus, for phase I of C-SAP participation as a CoI in the evaluation of CARTOSAT-1 data for test site TS5 (Mausanne-les-Alpilles, France) has been agreed upon.
For phase I of C-SAP no explicit exterior and interior orientation data of CARTOSAT-1 have been given. Instead, rational polynomial functions (RPC) are provided by the distributing Indian agency as a universal sensor model for each scene. Thus, only the inherent orientation accuracy of the RPC models is established by comparison to the available ground truth. Ground control points are used to correct the RPC (bias correction and also affine transformations). The resulting various residuals are assessed and commented. From these first investigations it can be seen that the offset of the original RPC is in the order of kilometres which was not expected. Bias correction ends up with residuals at ground control points (GCP) in the order of several pixels showing also systematic behaviour. This leads to the conclusion that RPC have to be corrected with affine transformations. The latter lead to residuals in the order of 1 pixel which is satisfactory for the start of investigations. DSM accuracies are assessed via residuals in forward intersection (tie point cloud from matching) and through calculation of 3D shifts between reference DEM and calculated DSM by least squares adjustment (full DEM/DSM comparison). Using affine transformation correction of RPC a standard deviation of the DEM/DSM height differences of 3-4 m is achieved which is very good when taking the inherent DEM/DSM differences into account.

1. INTRODUCTION

1.1 General DLR stereo scanner background

DLR is engaged in 3-line stereo scanner development since 1980 when ISRO offered to fly such a DLR camera on SROSS-I satellite to be launched by Indian ASLV rocket in 1988. The camera has been built and the German photogrammetric community and also ISRO/SAC could exploit airborne 3-line scanner imagery of an airborne camera model from 1986 onwards (Lehner&Gill 1992, Heipke et al., 1996). Unfortunately, the camera did not reach space due to launch vehicle failures but Indian and German scientists profited much from the cooperation. Anyhow, the ground resolution of about 70 m together with the at that time very restricted measurement possibilities for exterior orientation would have allowed to derive coarse digital surface models (DSM) only.
DLR in subsequent years concentrated on the German 3-line scanner MOMS-02 which was successfully flown as MOMS-02/D2 instrument on space shuttle mission D2 in 1993 and as MOMS-2P on the Russian space station Mir from 1996 till 1999. MOMS mission brought the development of a MOMS stereo work station at DLR through cooperation of DLR with several German universities. (Seige et al, 1998)
As in spite of many negotiations a follow-on project (MOMS-03) did not come true DLR applied its evaluation experience to upcoming foreign missions. The next along-track stereo scanner in space was the HRS instrument on SPOT-5. DLR took part as a PI in the HRS scientific assessment program 2003-4 (Reinartz et al, 2006). Special additions to the software system at DLR have been made for stereo IKONOS-2 and QuickBird images (Lehner et al, 2005) along the lines given in various papers (e.g. Grodecki et al, 2004).

1.2 Special interest in CARTOSAT-1

As optical stereo data from space are by far not meeting the demand – since the launch of CARTOSAT-1 (IRS-P5) in May 2005, the DLR institute was eagerly waiting for a chance to evaluate this kind of 2-line stereo data with a very interesting resolution of 2.5 m. This resolution should be adequate for many 3D mapping tasks.
C-SAP has now given this possibility. For C-SAP DLR proposed to take the ground truth already available from the PI role in SPOT-HRS-SAP for Bavarian and Catalonian test sites. As this did not come true in time for phase I we got the chance of a CoI-ship for test site 5, very friendly welcome by the JRC team which delivered excellent ground truth.

1.3 Investigations presented in this paper

Investigations are based on delivered image data and RPC.

Matching is performed with DLR software to give mass tie points.

Relative RPC correction can be done based on forward intersection using best quality tie points from matching. This gives the possibility to generate DSM and orthoimages fitting to each other in the absence of ground control (3D projections etc. can be generated.)

Absolute RPC correction is based on ground control points (GCP) (Mausanne-les-Alpilles). Bias correction only already leads to results with accuracy of about 2-3 pixel. Residual vectors for the GCP indicate systematic distortions to be still present. Thus, higher order correction of residuals is done (affine transformation) leading to substantial further improvements seen via residual statistics and comparison to reference DEM.

As a general comment on CARTOSAT-1 data it can be stated that the MTF of aft-looking sensor is much better than the MTF of the fore-looking sensor. This can be seen already by pure visual inspection and should be quantified in phase II (if not yet done). Of course, matching results are influenced substantially.

2. CARTOSAT DATA AND GROUND TRUTH

2.1 Test site 5 – Mausanne-les-Alpilles

2 CARTOSAT-1 stereo pairs are provided – basic parameters are given in table 2-1 (with abbreviations for the images). DEM and ground control points are provided by JRC.

Table 2-1: CARTOSAT-1 stereo pairs Mausanne-les-Alpilles (MA/F1: 31Jan06, MA/F2: 06Feb06)

image	alt	head	incid.	c-roll	c-pit	c-yaw
MA1	625.8	194.0	33.04	-13.6	-0.01	2.25
MF1	625.5	194.0	33.01	-13.6	-0.01	2.10
MA2	625.9	194.1	29.17	4.01	0.03	2.70
MF2	626.5	194.1	29.18	4.01	0.04	2.56

A reference DEM of most of the area of the test site 5 and ground control point coordinates measured by GPS survey and corresponding image chips and photos of the measurement configurations have been delivered by the PI of test site 5 from JRC.

2.2 Test site 10 - Catalonia

A stereo pair is provided – some details are given in table 2-2. A DEM and orthoimages with scale 1:5000 are provided by ICC.

Table 2-2: Catalonian CARTOSAT-1 stereo pair (01Feb06)

image	alt	head	incid.	c-roll	c-pit	c-yaw
CA	625.2	193.7	29.07	0.10	0.04	2.73
CF	625.8	193.7	29.07	-0.10	0.04	2.59

2.3 Matching for tie point generation

Hierarchical intensity based matching as implemented into XDibias image processing system of DLR consists of two major steps.

In a first step the matching process uses a resolution pyramid (Lehner&Gill, 1992; Kornus et al., 2000) to cope even with large stereo image distortions stemming from carrier movement and terrain. Large local parallaxes can be handled without knowledge of exterior orientation (which is - or was: it has improved much in the near past - often not available with sufficient accuracy). The selection of pattern windows is based on the Foerstner interest operator which is applied to one of the stereo partners. For selection of search areas in the other stereo partner(s) local affine transformations are estimated based on already available tie points in the neighborhood (normally from a coarser level of the image pyramid). Tie points with an accuracy of one pixel are located via the maximum of the normalized correlation coefficients computed by sliding the pattern area all over the search area. These approximate tie point coordinates are refined to sub-pixel accuracy by local least squares matching (LSM). The number of points found and their final (sub-pixel) accuracy achieved depend mainly on image similarity and decrease with increasing stereo angles or time gaps between imaging. The software was originally devised for along-track 3-line stereo imaging (stereo scanners MEOSS and MOMS operated by DLR). Normally, the procedure can be executed fully automatically. In certain special cases (like cloudy images) a few (minimum 3) manually identified tie points have to be provided on the lowest resolution level of the image pyramid. The procedure results in a rather sparse set of tie points well suited for introduction into bundle adjustment and as an excellent source of seed points for further densification via region growing (second step).

The second step uses the region growing concept first published by Otto and Chau in the implementation of TU Munich (Heipke et al., 1996). It combines LSM with a strategy for local propagation of initial conditions of LSM.

Various methods for blunder reduction are used for both steps of the matching:

- Threshold for correlation coefficient
- 2-directional matching and threshold on resulting shifts of the coordinates
- Threshold on residuals (in image space) from forward intersection based on the rigorous modeling of the imaging process or on rational polynomial functions (RPC).

In areas of low contrast the propagation of affine transformation parameters for LSM in region growing leads to high rates of blunders. In order to avoid intrusion into homogeneous image areas (e.g. roof planes without structure) the extracted image chips are subject to (low) thresholds on variance and roundness of the Foerstner interest operator. This and the many occlusions found in densely built-up areas imaged with a large stereo angle create lots of insurmountable barriers for region growing. Thus, for high resolution stereo imagery the massive number of seed points provided by the matching in step one (image pyramid) turns out to be essential for the success of the region growing.

The numbers of tie points found and their sub-pixel accuracy is highly dependent on the stereo angle. A large stereo angle (large base to height ratio b/h) leads to poorer numbers of tie points and to lower accuracy in LSM via increasing dissimilarity of (correctly) extracted image chips.

3. RPC RELATIVE CORRECTION

RPC are relatively corrected using residuals of forward intersection for tie points from matching (carefully selected) to give a system of RPC to be able to generate fitting triples of

orthoimages and DSM. Normally, IKONOS-2 stereo pairs are delivered with zero mean residuals via relative bundle adjustment during RPC generation. QuickBird mean residuals reported in (Lehner et al, 2005) are in the same order as CARTOSAT-1 residuals given in table 3-1 for MA/F1. Anyhow, one has to do the matching for DSM generation and RPC relative correction can be based upon these stereo tie points (bias correction only when just applying mean residuals).

Table 3-1: residuals (pixel) from forward intersection with original RPC (after blunder reduction – residual threshold 0.5 pixel)

Image	row residuals		column residuals	
	mean	s	mean	s
MA1	-0.102	0.008	-28.919	0.132
MF1	0.070	0.005	29.978	0.134
MA2	0.009	0.001	-2.637	0.290
MF2	-0.010	0.001	2.699	0.291
CatA	0.013	0.001	-8.224	0.279
CatF	-0.014	0.004	8.481	0.279

At this stage many tie points have been rejected due to threshold 0.5 pixel for M2 and Cat cases (M1: 68/8484 – 0.8%, M2: 8676/25574 – 66.1%, Cat: 31980/58795 – 54.4%).

4. RPC ABSOLUTE CORRECTION

4.1 GCP measurement for test site 5

13 of the GCP measured by JRC have been identified in MA/F1 (060131) images. Image coordinates of MF1 have been adjusted in sub-pixel accuracy by multi-window LSM (6 window sizes from 17 to 27 – mean standard deviations in rows and columns for the 13 GCP and 6 window sizes were 0.11 and 0.08 pixel, respectively, being quite satisfactory).

4.2 Bias correction of RPC

Application of original RPC delivered with the images leads to the mean shift vectors given in table 4-1 (with statistics). Deviations of the mean shifts at the individual GCP locations are shown in figures 4-1 and 4-2. The systematic behaviour of these deviations indicate that pure bias correction of RPC is not sufficient. The large bias values in flight direction show that orbit/attitude determination is not current state of the art found in SPOT (DORIS system) and IKONOS/QuickBird (GPS) systems (see e.g. Reinartz et al, 2006, Eisenbeiss, 2004 and Ager, 2003). Direct georeferencing of CARTOSAT-1 data with errors of only a few pixels is therefore only possible with GCP.

Table 4-1: mean shifts for the GCP between measured and RPC based image coordinates and corresponding standard deviations (bias correction of RPC)

image	number	mean shift		s	
	of GCP	row	column	row	column
MA1	13	-2259.2	-780.0	1.99	2.84
MF1		-2159.3	-634.4	3.06	2.78

Table 4-2: shift parts of affine transformations and standard deviations of residuals for affine correction of RPC

image	number	shift part of aff.tr.		s of residuals	
	of GCP	row	column	row	column
MA1	13	-2253.7	-791.3	0.88	1.05
MF1		-2152.9	-629.9	0.92	1.02
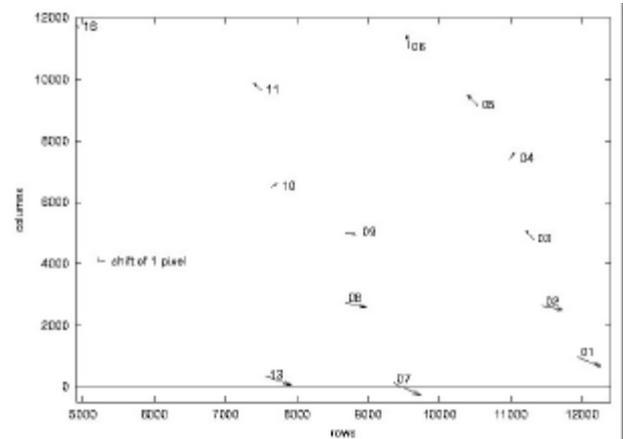
Figure 4-1: Deviations (factor 100 enlarged) from mean shifts vectors of measured versus RPC image coordinates of GCP in case MA1
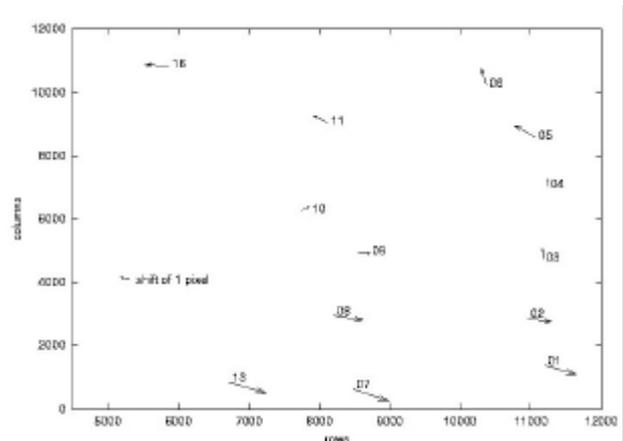
Figure 4-2: Deviations (factor 100 enlarged) from mean shifts vectors of measured versus RPC image coordinates of GCP in case MF1

4.3 RPC correction via affine transformation

Thus, correction via full affine transformation was added to the DLR software like recommended in quite some publications. The correction equations are as follows:

$$row = a_0 + a_1 RPC_{row} + a_2 RPC_{col}$$

$$col = b_0 + b_1 RPC_{row} + b_2 RPC_{col}$$

$$where \quad RPC_{row} \, and \, RPC_{col} \quad are \, the \, originally$$

$$provided \, rational \, polynomial \, functions$$

After estimation and application of these affine transformations the residuals at the 13 GCP are much reduced as shown in figures 4-3 and 4-4. The standard deviations of the residuals

are given in table 4-2 and drop to near 1 pixel (about factor 3 reduced when compared to table 4-1).

Table 4-3 shows the mean and the standard deviation of the height differences to JRC DEM within forward intersection for the case of bias and affine correction for the following sets of tie points for stereo pair MA/F1:

1. PS1: about 8500 carefully selected tie points with very good bi-directional LSM behaviour
2. PS2: about 3850000 tie points from region growing for full scenes with step size 3 in both directions
3. PS3: about 12628000 tie points from region growing for left upper quarter scene (6000 rows and columns) with step size 1 in both directions
4. PS4: about 7000000 tie points from region growing for lower right quarter scene (6000 rows and columns) with step size 1 in both directions
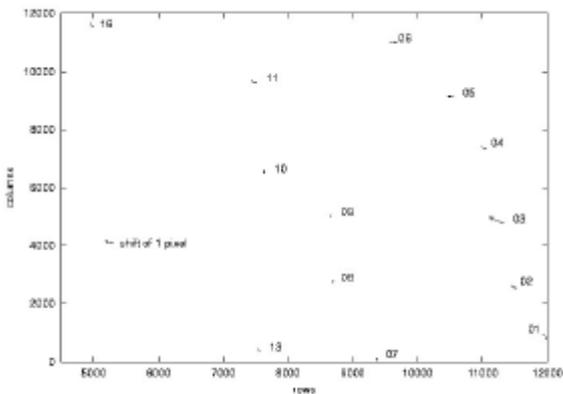
Figure 4-3: Deviations in pixel (factor 100 enlarged) of measured versus RPC image coordinates after affine transformation correction of RPC at 13 GCP (MA1)
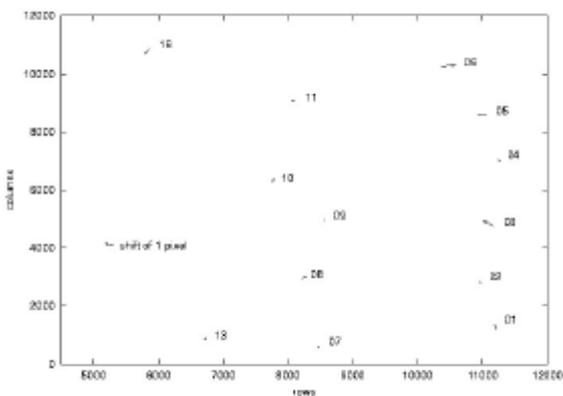
Figure 4-4: Deviations in pixel (factor 100 enlarged) of measured versus RPC image coordinates after affine transformation correction of RPC at 13 GCP (MF1)

Table 4-3: Means and standard deviations of height differences (m) produced by subtracting CARTOSAT DSM heights from reference DEM heights for point clouds derived by LSM

tie point set	Height differences to JRC DEM			
	RPC bias correction		RPC affine correction	
	mean	s	mean	s
PS1	-4.8	5.4	-3.7	2.4
PS2	-2.2	7.5	-2.6	5.5
PS3	-6.4	8.3	-3.1	7.8
PS4	2.5	9.5	-1.5	9.3

It can be clearly seen that in the case PS1 of very well defined matching points (surely not on complex objects like trees etc.) the drop in standard deviation is substantial (more than factor 2). In the other cases of region growing the reduction is not to be seen so easily because of the effects of object differences in DSM and reference DEM. There should be an individual investigation based on a classification of the landscape as presented in (Reinartz et al, 2006). This will be done in phase II of C-SAP.

Interpolation of the point clouds PS2-4 was done with DLR software described in (Hoja et al, 2005). The 3D shifts between the calculated regular DSM sets and the JRC reference DEM are shown in table 4-4. The DEM has hilly parts and also very flat ones with many lines of trees and built-up areas. In the short time of phase I of C-SAP no distinction could be made of the various classes of land use. Thus, results in table 4-4 are supposed to be biased by the distinct differences in object presentation between a DSM and a DEM, especially because no rotations between the digital elevation models are estimated. The estimated lateral shifts are only partly reduced when comparing bias and affine correction of RPC. Standard deviations of height differences are always reduced.

Table 4-4: Estimation of DSM shifts (in meter) versus reference DEM via least squares adjustment for DSM interpolated from the point sets PS2-4 for the 2 cases: forward intersection using bias or affine corrected RPC; s z (m) gives the standard deviation of height differences after application of the 3D shift (dx, dy, dz)

| DSM from	3D shift bias correction				3D shift affine correction			
	dx	dy	dz	s z	dx	dy	dz	s z
PS2	2.0	-3.0	-1.4	6.9	-5.9	-1.8	-1.9	3.5
PS3	6.9	-1.7	-6.5	4.7	-5.2	-4.3	-2.5	3.7
PS4	3.6	-27	2.9	4.0	-2.3	-15	-0.9	3.0

Figure 4-5 shows a 3D view generated from DSM and orthoimage in case PS2 with affine correction of RPC. Details can be seen in figure 4-6. It can be seen that rows of trees and houses are at least partly modelled.

5. CONCLUSIONS

Of the 3 CARTOSAT-1 stereo pairs mentioned in this paper because of shortage of time only one stereo pair for test site 5 (Mausanne-les-Alpilles, France, PI: Dr. Simon Kay, Agrifish Unit of the Institute for Protection and Security of the Citizen of the Joint Research Centre of the European Commission,

Ispra, Italy) has been more thoroughly studied. Thus, results reported in the paper and summarized below should be considered as first insights to be consolidated during phase II of C-SAP.

Large residuals in the order of kilometres have been found with original rational polynomial functions (RPC). Bias correction of RPC leaves residuals of several pixels which show systematic effects. The latter can be removed by applying a full affine transformation for the correction of the RPC. The standard deviations of the residuals at the GCP drop to about 1 pixel (which may be near to the identification accuracy of the GCP, tie point coordinates of GCP are registered with sub-pixel accuracy to each other via local least squares matching). Comparisons of the generated DSM with the JRC reference DEM via estimation of 3D shifts result in standard deviations of the height differences of 4-6 meters for bias correction and 3-4 meters for affine correction of RPC. This should be ranked as a nice result because no object classification in terms of DSM/DEM differences is applied which should be done in phase II of C-SAP.
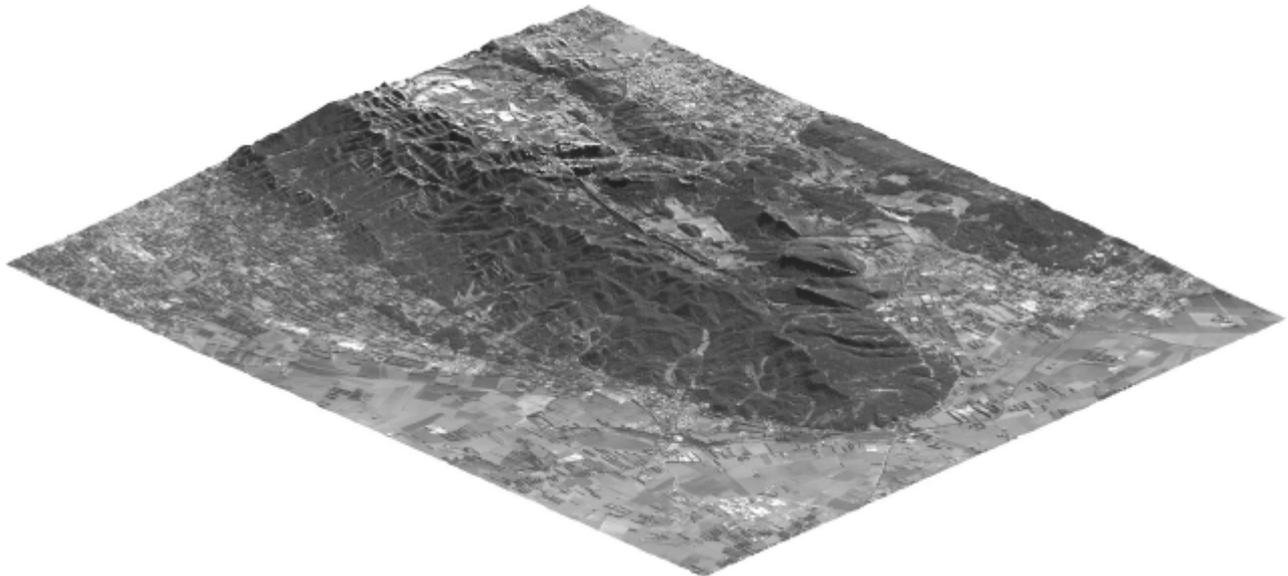
Figure 4-5: 3D view generated from DSM from point set PS3 and orthoimage of aft-looking sensor's scene produced with affine corrected RPC

References from Journals:
Heipke, C., Kornus, W., Pfannenstein, A., 1996. The evaluation of MEOSS airborne 3-line scanner imagery – processing chain and results, Photogrammetric Engineering and Remote Sensing, Vol. 62, No. 3, pp. 293-299

Reinartz, P., Müller, Rupert, Lehner, M., Schroeder, M., 2006: Accuracy Analysis for DSM and orthoimages derived from SPOT HRS stereo data using direct georeferencing, ISPRS Journal of Photogrammetry & Remote Sensing 60, pp. 160-169

References from Other Literature:
Ager, T. P., 2003: Evaluation of geometric accuracy of Ikonos imagery, SPIE 2003 AeroSense Conference, Orlando, Florida, USA

Eisenbeiss, H., Baltsavias, E., Pateraki, M., Zhang, L., 2004. Potential of Ikonos and Quickbird imagery for accurate 3D point positioning, orthoimage and DSM generation. International Archives of Photogrammetry, Vol 35, Part B, 20th ISPRS Congress, Istanbul

Grodecki, J., Dial, G., Lutes, J., 2004. Mathematical Model for 3D feature extraction from multiple satellite images described by RPCs. ASPRS Annual Conference Proceedings, Denver, Colorado, USA

Hoja, D., Reinartz, P., Lehner, M., 2005: DSM Generation from High Resolution Satellite Imagery Using Additional Information Contained in Existing DSM. Proceedings of the ISPRS Hannover Workshop 2005 High Resolution Imaging for Geospatial Information, Hannover, Germany

Lehner M., Gill, R.S., 1992: Semi-Automatic Derivation of Digital Elevation Models from Stereoscopic 3-Line Scanner Data, *IAPRS,* Vol. 29, part B4, Commission IV, pp. 68-75, Washington, USA

Lehner, M., Müller, Rupert, Reinartz, P., 2005: DSM and Orthoimages from QuickBird and Ikonos Data Using Rational Polynomial Functions, Proceedings of "High Resolution Earth Imaging for Geospatial Information", May 17-20, Hannover, Germany

Seige, P., Reinartz, P., Schroeder, M., 1998: The MOMS-2P mission on the MIR station, *IAPRS,* Vol. 32, Part 1, pp. 204-210, Bangalore, India (see also http://www.nz.dlr.de/moms2p)

Figure 4-6: Detail of figure 4-5